Advanced Design of a Robust and Effective EMI Detector for Wired Communication Channels

Hasan Habib, *Member, IEEE,* Tim Claeys, *Member, IEEE,* Guy A. E. Vandenbosch, *Fellow, IEEE,* and Davy Pissoort, *Senior Member, IEEE*

***Abstract*—In this letter, an advanced design of an electromagnetic interference detector for wired communication channels is proposed and analysed. A Monte-Carlo based simulation framework is used to evaluate the performance of the EMI detector under harsh electromagnetic environments. Based on this analysis, it is concluded that the proposed advanced EMI detector works effectively as long as the two involved data transmission lines are sufficiently close to each other.**

***Index Terms*—EMI, EMC, Electromagnetic Resilience, Risk Management, Bit Error Detection**

I. Introduction

Sophisticated applications such as autonomous vehicles, Industry 4.0 and the Internet of Things (IoT) heavily rely on complicated electric, electronic or programmable electronic (E/E/PE) devices and require particular focus on the dependability of the internal communication channels. IEEE Std 1848-2020 [1] proposes many hardware- and software-based techniques to reduce the risks related to the impact of bit errors induced by electromagnetic disturbances (EMDs) in such communication channels [2], [3]. Recent research has demonstrated that these hardware and software techniques can be quite effective, but specific scenarios have also been revealed in which their performance is still inadequate for safety-critical applications. Therefore, additional techniques and measures have to be added to reduce risks even further [4].

There was a need to develop a device that could detect the presence of an EMD in a communication channel along with its impact on the transmitted data over that channel. Existing electromagnetic interference (EMI) sensors detect the presence of an EMD regardless of its impact on the system. Examples of these include detectors for intentional EMI [5], an antenna-based Ultrawideband EMD detector [6] and field strength probes to estimate the EM field strength [7]. However, only detecting the presence of an EMD can be problematic for a safety-critical system that requires high availability, as there are cases when EMD is present but it is not causing any actual interference within the communication channel. Indeed, a typical reaction to the detection of an EMD would be to switch the system to a minimum risk state or safe state, which in many cases would mean that the system is shut down to avoid fatal errors. However, one doesn't want this to happen too often unnecessarily as this significantly reduces the system's availability.

The research leading to these results has received funding from the European Union's Horizon 2020 research and innovation programme under the Marie Skłodowska-Curie Grant Agreement No 812.790 (MSCA-ETN PETER). This publication reflects only the authors' view, exempting the European Union from any liability. Project website: http://etn-peter.eu/.

Software-based techniques, primarily error detection codes (EDCs), are currently used for bit error detection due to EMI, as mentioned in IEEE 1848-2020 [1]. However, they necessitate redundant data transmission and additional computation. Furthermore, EDCs need the transmission of data blocks to detect bit errors, adding a significant delay to the system. In [8], a comparator-based design was proposed. It uses a simple comparator to detect bit errors due to EMI in an inverted pair of data transmission lines. However, an in-depth analysis revealed that this comparator-based detector failed to detect when EMI inverts the transmitted data in both data transmission lines [4]. Therefore, a new design of an EMI detector based on an Adder and Subtractor (A&S EMI detector) was proposed in [4]. This design also employed an inverted pair of data transmission lines but used both the sum of and difference between the voltages at the receiver end to judge about the occurrence of EMI. The detector's performance in [4] and [9] was significantly better than the comparator-based design in [8]. However, it still failed to detect bit errors caused by EMI when the frequency of the EMD happened to be equal to or close to an integer multiple of the EMI detector's internal sampling frequency. In [10], it was proposed to combine the A&S EMI Detector with field strength probes, but the exact placement of these field strength probes for optimal performance is challenging. Therefore, this solution might not be so practical, especially when the communication channel is electrically long.

This letter proposes the design of an Advanced EMI detector that aims to detect bit-wise disturbances in the transmitted data due to EMI in all possible scenarios. The remainder of this letter is organized as follows. Section II discusses the theoretical principles behind the design of the Advanced EMI detector. Section III assesses the performance of the Advanced EMI detector. Finally, Section IV draws concluding remarks.

II. Design and Working Principle

The design of the Advanced EMI detector is proposed in Fig. 1. It receives a signal from the reciver end of an inverted pair of data transmission lines. To determine the presence of EMI, the Advanced EMI detector processes the received samples and aims to generate a warning when an EMD actually disturbs the transmitted data. The Advanced EMI detector oversamples each bit three times and uses the worst-case sample, i.e., the one with the largest induced voltage, to determine if a warning needs to be raised. The overall design uses the Adder-part of the A&S EMI detector and also adds a phase shift in the Adder-part to a second detector channel.

In our study, the data is transmitted using unipolar Non-Return-to-Zero-Level (NRZ-L) encoding, where a binary

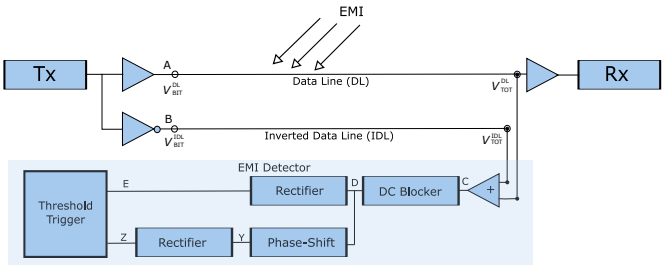

Fig. 1: Block Diagram of the Advanced EMI Detector

'1' is represented by 0.5 V and a '0' by 0 V. Both the data and inverted data transmission lines transmit the data with a fixed frequency f_{BIT}. The receiver Rx samples the received bit in the middle of the bit and decodes voltages higher than 0.33 V as '1', lower than 0.16 V as '0'. If a voltage is between 0.16 V and 0.33 V the bit is automatically considered as a bit-error in our study (worst-case analysis).

The Advanced EMI detector aims to determine whether or not a received signal has been disturbed by an EMD. For this purpose, it uses two circuits called the Adder and the Adder with a phase-shift, as shown in Fig. 1. In general, when EMI is not present, the sum of voltages from data and inverted-data lines is equal to a constant V_{DC}. The DC blocker removes the constant voltage V_{DC} and the rectifier rectifies the residual signal, which may be zero volts. However, in the presence of EMD, the sum of voltages from both lines is not equal to the constant V_{DC}. The DC blocker subtracts the constant V_{DC} and the remaining difference in voltage is further rectified. The Advanced EMI detector generates a warning if the rectified voltage is greater than a pre-defined threshold voltage $V_{\text{thresh}}^{\text{det}}$.

If there is a negligible distance between two data transmission lines, the phase difference ϕ between both lines is almost zero, and an EMD will induce an equal voltage in both data transmission lines and the Adder would very efficiently detect the presence of an EMD in these cases. However, practically it is not possible to have two co-located data transmission lines. Hence, there will always be a phase difference between both transmission lines. For large phases differences, the Adder might fail to detect EMI. The phase difference of EMD-induced voltages can induce voltages of opposite polarity in data transmission lines. The simple Adder fails to detect when the sum of opposite-polarity voltages is less than the pre-defined threshold voltage $V_{\text{thresh}}^{\text{det}}$. Since the polarity of the EMD induced voltage is a function of its phase, shifting the phase of the added voltage can also shift the sum so that it is greater than $V_{\text{thresh}}^{\text{det}}$, thereby eliminating the possibility of a failed detection. Therefore, a phase-shifter is added to shift the sum of the signal from both data transmission lines. In most cases, the frequencies of the EMD are unknown; thus, a phase shifter for the range of unknown frequencies can be implemented using the concepts of a frequency-independent phase shifter given in [11], [12].

Overall, the Advanced EMI detector processes the signal twice, with and without the phase-shift. In this letter, zeros of a sinusoidal signal are shifted to the maxima by adding a 90° phase-shift. Fig. 2 illustrates the impact of introducing a phase shift to a time domain signal. The analysis reveals that by shifting the phase of an undetectable signal at the sample points, the signal can become detectable. However, when there is a very large phase difference, i.e., more than 90°, the sum of the EMD induced voltages between the data transmission lines, even with a phase-shift, may remain lower than the pre-defined threshold voltage $V_{\text{thresh}}^{\text{det}}$, and the detector may fail to generate a correct warning.

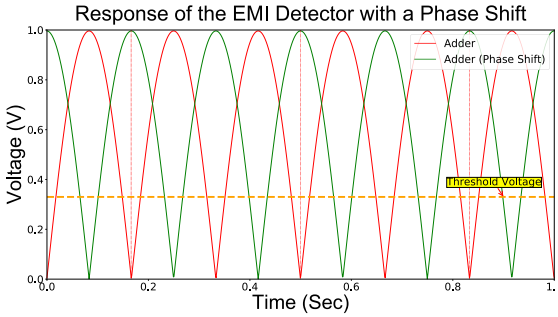

Fig. 2: EMD Induced voltage, with and without phase-shift

The Advanced EMI detector will generate a warning when the processed EMD induced voltage, with or without phase-shift, is greater than the pre-defined threshold voltage $V_{\text{thresh}}^{\text{det}}$ at any of sample points over one bit. The overall design generates a warning when either the Adder with or without phase-shift has been triggered.

III. Performance Evaluation

The performance of the Advanced EMI detector is analysed in a reverberating EM environment using the Monte-Carlo-based simulation framework, previously used in [13]. This incorporates a large number of occurring reflections comparable to a reverberation room.

a) Geometry Under Study: The study is performed using a well-defined geometry of data transmission lines as shown in Fig 3. A single PCB with dimensions of 10 cm by 16 cm and a thickness of 1.6 mm is used for the analysis. The PCB uses an FR4 substrate, and the bottom layer is covered with a complete ground plane. The PCB uses two data transmission lines, and both are 3 mm wide, having a characteristic impedance of 50 ohms. The distance between the parallel traces is 10 mm from centre to centre.

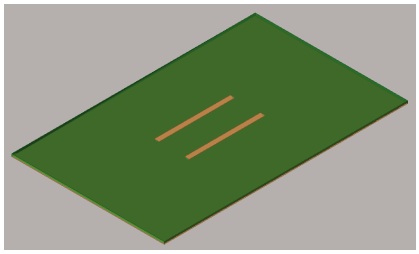

Fig. 3: Geometery of the PCB Design

b) Simulations: The finite difference time domain (FDTD) solver from Keysight Technologies' PathWave is used to perform the full-wave simulations in this letter. All post-processing analyses were carried out utilizing an in-house developed simulation framework. The applied EMD in the simulation framework replicates a reverberating environment

and incorporates a large number of reflections comparable to a reverberation room environment. The simulation framework incorporates the induced voltages due to an incoming EMD, as well as the signal integrity of the data transmission lines. The S-parameters between the transmitter and the receiver take into account the actual response of the data transmission lines, including characteristic impedance, resonances, time delay from one end to the other, and mutual coupling between data transmission lines [14]. In the simulations, 100 random bits are transmitted through the data transmission lines. The rise and fall times of the bit transitions have been adjusted to 0.1 nanoseconds. A reverberating environment is modeled by N=200 superimposed plane waves, each with a random polarization and angle of arrival. The superimposed waves require a normalization, so field strength is normalized by $\mathrm{E}_N = \mathrm{E}_0/\sqrt{N}$ [14]. To account for the statistically changing characteristic of a reverberating environment, simulations are repeated for M=10000 distinct sets of such plane waves. The design of the Advanced EMI detector is implemented in Python, which acquires the transmitted signal from the receiver end of the data transmission lines. Each bit is sampled multiple times, i.e., 360. The samples are delayed according to the EMD frequency to attain the 90 degrees phase shift for the EMD induced voltage.

The impact of the EMD induced voltage on the transmitted data is always dependent on the voltages used for the transmission of data. Therefore, the EMI detector's response is analysed by using a Signal-to-Interference ratio (SIR). The SIR is defined as the ratio between the root mean square value of the actual signal and a root mean square value of the EMD induced voltage, i.e, $\mathrm{SIR} = 20 \cdot \log_{10}\left(V_{\mathrm{BIT}}^{\mathrm{RMS}}/V_{\mathrm{EMD}}^{\mathrm{RMS}}\right)$.

In the simulation framework, the SIR is calculated by using the average RMS induced voltage for a particular incident field strength. This is done by first evaluating the RMS induced voltage for each reverb waveform. Afterwards, the average RMS induced voltage is calculated by averaging it for M waveforms. The analysis is performed at different frequency ratios, which can be defined as the ratio of an EMD frequency to a bit frequency, i.e., $f_{\mathrm{ratio}} = f_{\mathrm{EMD}}/f_{\mathrm{BIT}}$

1) Results: This subsection shows the results of the analysis performed to evaluate the Advanced EMI detector. The condition assessment definitions introduced in [15] are used to analyse the performance of the Advanced EMI detector. These definitions are used to classify the received signal based on its impact on channel health and the system. These definitions classify the response of the EMI detector as Data True Positive (DTP), Channel True Positive (CTP), Data False Positive (DFP), Channel False Positive (CFP), Channel True Negative (CTN), and Channel False Negative (CFN). In the results, ideally, the percentage of DTPs (green region) should be as high as possible because in these the strength of the EMD is not high enough to disturb the transmitted signal and the EMI detector does not generate a warning. The occurrence of DFPs (yellow region) should be as low as possible as they compromise availability. They appear when the EMD is present but not strong enough to disturb the transmitted data, and the EMI detector still generates a warning. In the presence of EMI, CFPs (orange region) and CTNs (salmon region) should occur as these are the cases when EMD can disturb the transmitted data and the EMI detector generates a warning. On the other hand, CFNs(red) should not be present as they cause safety risks. They occur when an EMD corrupts the transmitted data, but the EMI detector fails to generate a warning.

Fig. 4 shows the response of the Advanced EMI detector for the EMD frequency equal to the bit frequency of 500MHz, representing $f_{\mathrm{ratio}} = 1$. It can be observed that bit error rate (BER) increases as SIR decreases, and the Advanced EMI detector detects EMI across the entire SIR range.

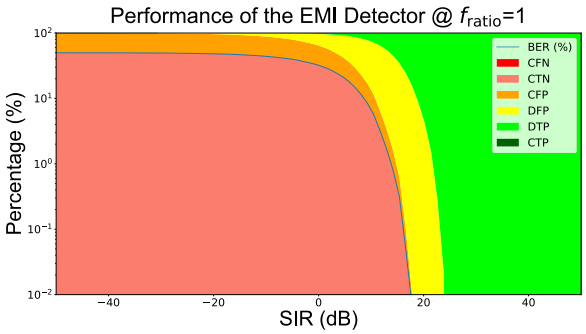

Fig. 4: Response of the EMI Detector at f_{EMD} = 500 MHz and f_{BIT} = 500 MHz, distance between data transmission lines = 10 mm

In addition, an analysis is performed for the f_{ratio}=3, in which a bit frequency of 166.666 MHz and the EMD frequency of 500 MHz is used. Results in Fig. 5 shows that the Advanced EMI detector can detect EMI at frequencies multiple of the sampling rate. The A&S EMI detector given in [4] was not able to detect EMI for some cases at f_{ratio}=3.

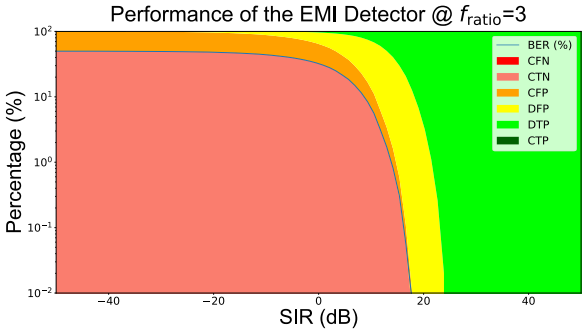

Fig. 5: Response of the EMI Detector at f_{EMD} = 500 MHz and f_{BIT} = 166.666 MHz, distance between data transmission lines = 10 mm

Enlarging the distance between data transmission lines at the same EMD frequency or increasing the EMD frequency while keeping the distance between data transmission lines constant can increase the phase difference of EMD-induced voltage in data transmission lines. Therefore, in order to analyse the response of the Advanced EMI detector when the phase difference of an EMD induced voltage between data transmission lines is substantial, the distance between data transmission lines is increased from 10 mm to 40 mm at the same EMD frequency as used in Fig. 5. The results in Fig. 6 show that the Advanced EMI detector fails to detect EMI in some cases.

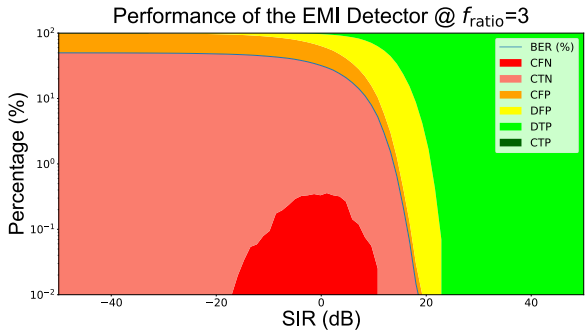

Fig. 6: Response of the EMI Detector at f_{EMD} = 500 MHz and f_{BIT} = 166.666 MHz, distance between data transmission lines = 40 mm

Furthermore, the impact of distance between the data transmission lines on the performance of the A&S and the Advanced EMI detector is analysed. This analysis is performed for f_{ratio}=3, N = 200 and M = 1000, as given in Fig. 7. The results show the total percentage of CFNs for the same SIR range as in Fig. 4-6 The results show that the A&S EMI detector generates CFNs when the distance between data transmission lines is increased from 4mm to 6mm. The distance between data transmission lines and the phase difference of the EMD induced voltage is directly proportional. Therefore, the number of CFNs rises as the distance increases. On the other hand, the Advanced EMI detector does not generate CFNs until the distance between data transmission lines is greater than 26mm. Overall, the findings demonstrate that when the distance between data transmission lines is not very large, the Advanced EMI detector can be used effectively.

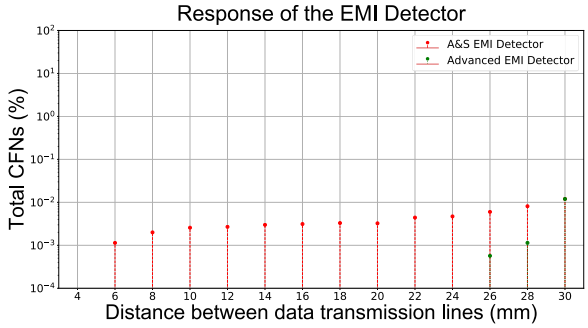

Fig. 7: Response of the EMI Detector at f_{EMD} = 500 MHz and f_{BIT} = 166.666 MHz, distance between data transmission lines increased from 4 mm to 30 mm

IV. CONCLUSION

This paper proposes the Advanced EMI detector that can detect bit errors due to EMI in closely placed data transmission lines. The primary aim of the design of the EMI detector is to eliminate CFNs since this is a top priority in terms of safety. This is achieved by using an additional phase-shift block along with the Adder.

The design is assessed under a harsh EM environment by using a Monte-Carlo based simulation framework. The results show that the newly proposed Advanced EMI detector can detect EMD induced bit errors in all considered cases, meaning that no CFNs occur as long as the two data transmission lines are sufficiently close to each other, i.e., an EMD is not inducing a voltage with a very large phase difference between data transmission lines (more than 90 degrees). In contrast, the previously proposed A&S EMI detector did suffer from CFNs for specific values of the ratios between the EMD's frequency and the bit frequency, even for the closely spaced data transmission lines.

REFERENCES

[1] "IEEE Std 1848-2020 - IEEE Standard for Techniques and Measurement to Manage Functional Safety and Other Risks with Regards to Electromagnetic Disturbances," 2020. [Online]. Available: https://standards.ieee.org/standard/1848-2020.html

[2] S. Van De Beek and F. Leferink, "Robustness of a TETRA base station receiver against intentional EMI," *IEEE Transactions on Electromagnetic Compatibility*, vol. 57, no. 3, pp. 461–469, June 2015.

[3] J. S. Bilodeau, A. Bouzouane, B. Bouchard, and S. Gaboury, "An experimental comparative study of RSSI-based positioning algorithms for passive RFID localization in smart environments," *Journal of Ambient Intelligence and Humanized Computing*, vol. 9, no. 5, pp. 1327–1343, Oct 2018. [Online]. Available: https://link.springer.com/article/10.1007/s12652-017-0531-3

[4] H. Habib, T. Claeys, D. Vanoost, and G. A. E. Vandenbosch, and D. Pissoort, "Development of an EMI detector based on an inverted data pair with reduced number of false negatives," in *2020 International Symposium on Electromagnetic Compatibility - (EMC EUROPE)*.

[5] J. F. Dawson, I. D. Flintoft, P. Kortoci, L. Dawson, A. C. Marvin, M. P. Robinson, M. Stojilović, M. Rubinstein, B. Menssen, H. Garbe, W. Hirschi, and L. Rouiller, "A cost-efficient system for detecting an intentional electromagnetic interference (IEMI) attack," in *IEEE International Symposium on Electromagnetic Compatibility*, Oct 2014, pp. 1252–1256.

[6] S. Ghosh and A. Chakrabarty, "Ultrawideband performance of dielectric loaded T-Shaped monopole transmit and receive antenna/EMI sensor," *IEEE Antennas and Wireless Propagation Letters*, vol. 7, pp. 358–361, 2008.

[7] F. Leferink, "Fast, broadband, and high-dynamic range 3-d field strength probe," *IEEE Transactions on Electromagnetic Compatibility*, vol. 55, no. 6, pp. 1015–1021, Dec 2013.

[8] J. Lannoo, A. Degraeve, D. Vanoost, J. Boydens, and D. Pissoort, "Effectiveness of inversion diversity to cope with EMI within a two-channel redundant system," in *2018 IEEE International Symposium on Electromagnetic Compatibility and 2018 IEEE Asia-Pacific Symposium on Electromagnetic Compatibility (EMC/APEMC)*, May 2018, pp. 216–220.

[9] H. Habib, T. Claeys, J. Lannoo, D. Vanoost, G. A. Vandenbosch, and D. Pissoort, "Implementation of inverted-pair EMI detector using a monte-carlo based simulation framework," in *2020 29th International Scientific Conference Electronics, ET 2020 - Proceedings*. Institute of Electrical and Electronics Engineers Inc.

[10] H. Habib, T. Claeys, R. Vogt-Ardatjew, B. van den Berg, G. A. Vandenbosch, and D. Pissoort, "Combining fast field probes with an EMI detector to reveal bit errors induced by electromagnetic disturbances," accepted for publication in 2022 IEEE International Symposium on Electromagnetic Compatibility (EMC Europe), 2022.

[11] K. Miyaguchi, M. Hieda, K. Nakahara, H. Kurusu, M. Nii, M. Kasahara, T. Takagi, and S. Urasaki, "An ultra-broad-band reflection-type phase-shifter MMIC with series and parallel LC circuits," *IEEE Transactions on Microwave Theory and Techniques*, vol. 49, no. 12, pp. 2446–2452, 2001.

[12] M. Madihian, K. Watanabe, and T. Yamamoto, "A frequency-independent phase shifter," *Journal of Physics E: Scientific Instruments*, vol. 12, p. 1031, 02 2001.

[13] J. Lannoo, D. Vanoost, J. Van Waes, J. Peuteman, J. Boydens, and D. Pissoort, "Effectiveness of frequency diversity to create EM-diversity in triple-modular redundant data transmission systems," *IEEE Transactions on Electromagnetic Compatibility*, vol. 63, no. 3, pp. 1–8, 2020.

[14] M. Magdowski, S. V. Tkachenko, and R. Vick, "Coupling of stochastic electromagnetic fields to a transmission line in a reverberation chamber," *IEEE Transactions on Electromagnetic Compatibility*, vol. 53, no. 2, pp. 308–317, 2011.

[15] T. Claeys, H. Tirmizi, H. Habib, D. Vanoost, and G. A. E. Vandenbosch, and D. Pissoort, "A system's perspective on the use of EMI detection and correction methods in safety critical detector," in *2021 International Symposium on Electromagnetic Compatibility - (EMC EUROPE)*.